International Scholarly Research Network
ISRN Signal Processing
Volume 2011, Article ID 254597, 8 pages
doi:10.5402/2011/254597

Research Article

Iterative Channel Estimation for Nonbinary LDPC-Coded OFDM Signals

Giacomo Bacci, Marco Della Maggiora, and Marco Luise

Wireless Systems Engineering and Research (WISER) S.r.l., Via Fiume, 23, 57123 Livorno, Italy

Correspondence should be addressed to Giacomo Bacci, giacomo.bacci@wiser.it

Received 20 December 2010; Accepted 8 March 2011

Academic Editor: C. S. Lin

This work deals with the issue of channel estimation in the context of non-binary LDPC-coded OFDM systems over doubly selective multipath channels. In particular, we show how to derive an iterative Wiener-filter-based estimation method using both time and frequency channel correlation and considering the particular characteristics of the channel code. The proposed algorithm can use either soft information or hard decisions fed back by the decoder to refine the channel estimation, so as to improve the system performance at the expense of an increased receiver complexity. Simulation results under typical working conditions are presented to compare the performance of the proposed method with respect to classical techniques.

1. Introduction

The increasing demand for high-speed wireless communications calls for efficient technologies in terms of energy expenditure and bandwidth occupation. In the area of forward error correction (FEC) coding, LDPC codes over high-order finite Galois fields GF(q), termed nonbinary LDPC (NB-LDPC) codes, were shown to bear a potential compared to other techniques [1]. To mention a few, NB-LDPC codes show a lower error floor with respect to their binary counterpart (LDPC codes), while providing a steep waterfall region in terms of word error rate (WER) compared to convolutional turbo codes [2]. Although this feature comes at the expense of an increased complexity at the receiver, NB-LDPC coding can be considered as a viable technology for beyond-4G communication systems [2].

Wideband signals for high-speed digital communications over a wireless link suffer from distortions caused by multipath propagation. The potentiality on NB-LDPC can be fully exploited if we can adopt an iterative channel estimation technique based on the channel decoder information to mitigate the effects of channel selectivity. Recently, there has been a flurry of research in this field using the "turbo" principle [3, 4], that can be applied to ancillary signal detection functions whenever the channel decoder is iterative and/or soft-output. This approach, analogous to what turbo codes do in the field of data detection, is referred to as "turbo" equalization. In [5], an iterative channel estimation is applied to a turbo-coded pilot-aided BPSK system over flat-fading channels. This solution provides a significant improvement in the performance by iteratively estimating the channel, and using the estimate to decode the turbo code. One drawback of the proposed technique is the bit error rate (BER) floor level, which is about an order of magnitude higher than that achieved by a turbo-coded system with ideal BPSK detection. However, the authors suggest the use of the channel estimates from previously decoded frames to significantly reduce this floor. This approach is generalized in [6] to the case of double selectivity, using joint equalization and decoding. The channel estimator proposed in this work exhibits a reduced complexity and it is decoupled from the equalizer module. The proposed method is suitable for high-order modulations, channels with arbitrary power profile, and LDPC. Simulation results show a significant performance improvement in the case of iterative estimation as opposed to non iterative channel estimation.

Similar approaches are considered in [7, 8] assuming the channel fading rate to be high. The work in [7] considers systems where the channel is unknown and time varying, with a fading rate so high that tracking of the channel is required between the training sequences. The proposed algorithm adopts a separate channel estimator that runs in parallel and aids the equalizer to save complexity and to be suitable for a wide range of different equalization techniques. In [8], iterative channel estimation and equalization is derived for frequency-selective Rayleigh fading channels. The authors propose a soft input Kalman channel estimator, derived by restructuring the channel estimation problem as one of Kalman state estimation reflecting the soft information from the decoding process into the statistical description of the channel.

In the field of multicarrier systems, relevant results can be found in [9–11], which propose joint iterative data detection and channel estimation schemes for orthogonal frequency division multiplexing (OFDM) under double channel selectivity. In [9], pilot symbols are exploited at the first estimation stage. Then, the receiver performance is improved by properly incorporating the soft-information fed back by the decoder into the minimum mean square error (MMSE) channel estimator once it is available after the first iteration. To reduce the computational power, the authors propose an indirect MMSE iterative channel estimation and decoding (ICED) method based on the number of channel taps in the time domain. In [10], the authors adopt a Wiener filtering approach to produce the optimum estimate of channel response in the sense of MMSE. To improve the accuracy of channel estimation, soft information exchange between Wiener-filter-based channel estimator and error-correction decoder is employed. However, according to the authors' experiments, the iterative information exchange between Wiener-filter-based channel estimator and error-correction decoder does not always improve the receiver performance. In [11], the authors derive an iterative algorithm for joint data-detection and channel-estimation for OFDM systems, which includes iterative decoding at the receiver. This scheme considers a maximum *a posteriori*-based decoder that works in conjunction with an iterative channel estimator to provide more reliable information on the coded symbols.

The present paper elaborates on the turbo approach to derive an iterative channel estimation algorithm based on the soft output of the NB-LDPC decoder. Wiener filtering in the time and frequency domain is selected due to its simple implementation while producing the optimum estimate of the channel response in the sense of MMSE. To the best of the authors' knowledge, the impact of iterative channel estimation in the case of an NB-LDPC-coded system has not been investigated in the literature. The main scientific contribution of this document is the rigorous derivation of the proper way to include soft information in the channel estimation procedure. Instead of using ad hoc formulae, we show how the *a posteriori* average of the received channel symbol is exactly the piece of soft information that is required by the Wiener smoother for channel coefficient estimation. We consider an OFDM system operating over a time-varying frequency selective scenario, as described in Section 2, emphasizing the details that can be exploited to perform the channel estimation task. The proposed iterative estimation technique is derived in Section 3. Section 4 contains some simulation results, whereas some conclusions are drawn in Section 5.

2. System Description

This section describes the system model considered throughout this work, which is sketched in Figure 1. At the transmitter side, the binary source is segmented into words of $\log_2 q$ bits each, and each word is considered as the natural binary representation of a GF(q) symbol. A sequence u_ℓ, $\ell = 0, \dots, K-1$, of K such symbols represents our source message vector $\mathbf{u}$ and is encoded into a vector $\mathbf{c}$, containing N GF(q) symbols c_m, $m = 0, \dots, N-1$, by a NB-LDPC encoder with a rate K/N [1]. An NB-LDPC code is defined in terms of a very sparse pseudorandom parity check matrix, whose elements belong to a finite Galois field GF(q). The way the encoding process acts is very similar to that employed by binary LDPC codes. The fundamental difference is that all operations are to be intended in the GF(q) domain [2].

The transmission takes place over a multicarrier OFDM signal using N_s subcarriers. We consider an OFDM system, due to its robustness against fast frequency-selective fading, as experienced in advanced systems such as the IEEE 802.16 [12] and LTE [13] standards. To increase the frequency diversity of the signal, our set of encoded vectors $\mathbf{c}$ is mapped into quadrature amplitude modulation (QAM) symbols, and interleaved on a carrier basis. The coded symbols c_m, assuming one of the q possible values b_g, $g = 0, \dots, q-1$, are modulated onto the OFDM carriers and sent to the receiver. More in detail, the mapping function $\mu(\cdot)$ gathers a number N_G of coded GF symbols, with $N_G = \mathrm{lcm}(\log_2 M, \log_2 q)/\log_2 q$, and maps them onto a number N_Q of consecutive channel QAM symbols d_k, with $N_Q = \mathrm{lcm}(\log_2 M, \log_2 q)/\log_2 M$, where M is the QAM constellation order, and $\mathrm{lcm}(\cdot)$ stands for the least common multiple. In practice, this can be performed by expanding the coded symbols c_m in their binary images (each symbol providing $\log_2 q$ bits) and grouping them on a QAM symbol basis (i.e., with blocks of $\log_2 M$ bits). With this approach, the actual mapping that is used to associate QAM symbols to GF(q) symbols has practically no relevance on the coded bit performance—any random mapping gives the same result.

The OFDM signal undergoes a tapped-delay-line fading channel with additive white Gaussian noise (AWGN) and impulse response

$$h(t) = \sum_{i=0}^{N_p-1} \rho_i(t)\delta(t-\tau_i), \tag{1}$$

where $\delta(\cdot)$ is the Dirac's delta function, N_p is the number of multiple paths, τ_i is the delay of the ith path, and $\rho_i(t)$ is the realization of the ith path, with independent Gaussian-distributed real and imaginary parts with zero mean and variance $\sigma_i^2/2$, with σ_i^2 determined by the channel power delay profile (PDP). Both components of $\rho_i(t)$ have autocorrelation function $R_{\rho_i}(\tau) = \sigma_i^2/2 \cdot R_\rho(\tau)$, which depends on the maximum Doppler frequency f_D. Note that the powers $\{\sigma_i^2\}$ are normalized so as to fulfill $\sum_{i=0}^{N_p-1} \sigma_i^2 = 1$. The intercarrier interference (ICI) due to the time variation of the channel coefficients within one OFDM symbol block is not considered in this work. This simplifying assumption is consistent with the set of Doppler frequencies that is used

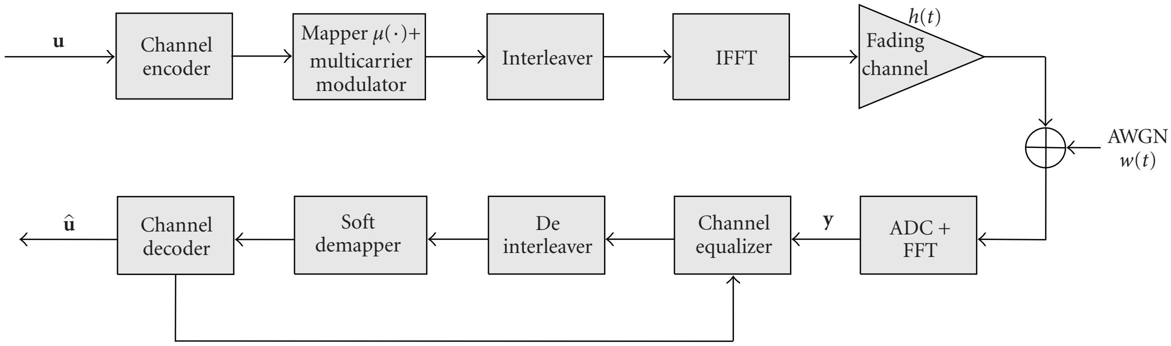

Figure 1: Block diagram of the system model.

in our numerical results (Section 4). The method described below can include the effects of ICI resorting to a Taylor expansion approach [14].

The fast Fourier transform (FFT) operation gives the vector $\mathbf{y}[n] = [y_1[n], \ldots, y_{N_s}[n]]$, where $y_k[n] = d_k[n]h_k[n] + w_k[n]$ is the kth received subcarrier of the nth OFDM symbol in the frequency domain, with $d_k[n]$ being the QAM symbol mapped on the kth subcarrier, $w_k[n]$ being the complex AWGN sample in the frequency domain with power $\sigma_w^2/2$ over each component, and $h_k[n] \triangleq \mathcal{H}(k\Delta f; nT_s)$ being the channel response over the kth subcarrier of the nth OFDM symbol, where $\mathcal{H}(f;t) = \mathcal{F}\{h(t)\}$ is the frequency response of the channel, Δf is the subcarrier spacing, and $T_s = 1/\Delta f$ is the OFDM symbol duration.

Figure 2 depicts the general overall architecture of the decoder/demodulator considered throughout the paper, expanding the bottom branch of the block diagram of Figure 1. Channel equalization is mandatory to mitigate the effect of channel selectivity. By extracting the pilot carriers embedded in the OFDM format from the vector $\mathbf{y}[n]$, we can obtain a rough estimate of the channel $\widehat{\mathbf{h}}[n] = \{\widehat{h}_k[n]\}_{k=1}^{N_s}$ in conjunction with an estimate of the noise power $\widehat{\sigma}_w^2$ (the latter is used by the soft demapper and possibly by the channel equalizer according to the equalization strategy). The equalizer processes $\mathbf{y}[n]$, and its output is sent to a deinterleaver after removing virtual and pilot carriers. The stream is then subdivided in chunks of N samples, corresponding to one codeword, and each chunk is sent to a soft demapper and finally to an NB-LDPC decoder. Decoding techniques for NB-LDPC codes can be borrowed by their binary counterparts by extending all operations to the field GF(q). The considered system adopts a simplified version [15] of the extended min-sum (EMS) algorithm [16] that produces a matrix $\mathbf{\Lambda}$ of *a posteriori* probabilities (APPs) for all coded GF(q) symbols. Using $\mathbf{\Lambda}$, we can obtain an estimate $\hat{\mathbf{u}}$ of the transmitted symbols and the soft/hard information to be fed back to the channel estimator, as described in the next section.

3. Iterative Channel Estimation

To improve the system performance, we can exploit the information from the NB-LDPC decoder to refine channel estimation. We can use either the soft information $\mathbf{\Lambda}$ or the hard decisions $\hat{\mathbf{u}}$ (in addition to pilots) to produce a further estimate $\widehat{\mathbf{h}}[n]$. In a recursive fashion, this new estimate is reused by the decoder, and a new decision on the transmitted symbols is taken. This work considers a Wiener-filter-based channel estimator, due to its simplicity of implementation while ensuring an optimum MMSE solution.

The linear causal MMSE estimator that provides an estimate of $h_k[n]$ in the time-frequency domain is given by

$$\widehat{h}_k[n] = \sum_{l=-L}^{L} \sum_{s=0}^{S} a_{k,ls} \cdot y_{k-l}[n-s], \quad (2)$$

where the number of coefficients (i.e., the order) of the Wiener filter is $(2L+1) \times (S+1)$, $\{a_{k,ls}\}_{l=-L,\ldots,L}^{s=0,\ldots,S}$ are the complex-valued Wiener filter coefficients, and $y_k[n]$ is the kth received subcarrier of the nth OFDM symbol. The filter coefficients can be rearranged in a $(2L+1) \times (S+1)$ matrix $\mathbf{A}_k$ and computed following the MMSE criterion:

$$\begin{aligned} \mathbf{A}_k &= \{a_{k,ls}\}_{l=-L,\ldots,L}^{s=0,\ldots,S} \\ &= \underset{\widetilde{\mathbf{A}}_k \in \mathbb{C}^{(2L+1)\times(S+1)}}{\arg\min} \; \mathbb{E}\left\{ \left| \widehat{h}_k[n] - h_k[n] \right|^2 \right\}, \end{aligned} \quad (3)$$

where $\mathbb{E}\{\cdot\}$ denotes expectation. For convenience of notation, it is worth restating the filter (2) as

$$\widehat{h}_k[n] = \operatorname{tr}\left(\mathbf{A}_{\mathbf{k}}^H \mathbf{Y}_k\right) = \operatorname{vec}(\mathbf{A}_k)^H \operatorname{vec}(\mathbf{Y}_k) = \mathbf{a}_{\mathbf{k}}^H \mathbf{y}_k, \quad (4)$$

where $(\cdot)^H$ denotes conjugate transposition; $\operatorname{tr}(\cdot)$ is the trace operator, $\operatorname{vec}(\mathbf{X})$ denotes the vectorization of the matrix $\mathbf{X}$ formed by stacking the columns of $\mathbf{X}$ into a single column vector, $\mathbf{a}_k \triangleq \operatorname{vec}(\mathbf{A}_k)$, $\mathbf{y}_k \triangleq \operatorname{vec}(\mathbf{Y}_k)$, and

$$\mathbf{Y}_k \triangleq \begin{bmatrix} y_{k-L}[n] & \cdots & y_{k+L}[n] \\ \vdots & \ddots & \vdots \\ y_{k-L}[n-S] & \cdots & y_{k+L}[n-S] \end{bmatrix} = \{y_{k,ls}\}_{l=-L,\ldots,L}^{s=0,\ldots,S}, \quad (5)$$

with

$$\begin{aligned} y_{k,ls} &\triangleq y_{k+l}[n-s] \\ &= d_{k+l}[n-s]h_{k+l}[n-s] + w_{k+l}[n-s] \end{aligned} \quad (6)$$

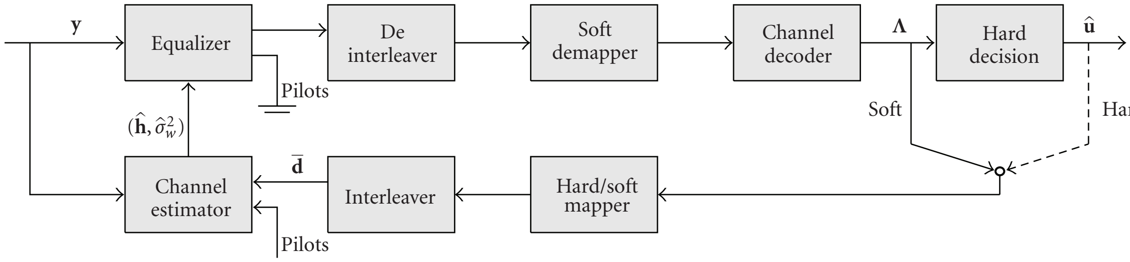

Figure 2: Structure of the NB-LDPC decoding stage using iterative channel estimation.

is a matrix containing the $(2L+1)\times(S+1)$ received samples in the frequency domain centered around the kth subcarrier of the current OFDM symbol and of the S past OFDM symbols. Using (6), $\mathbf{y}_k$ can be rewritten in a more convenient form:

$$\mathbf{y}_k = \boldsymbol{\Delta}_k \mathbf{h}_k + \mathbf{w}_k, \tag{7}$$

where $\boldsymbol{\Delta}_k \triangleq \text{diag}(\mathbf{d}_k)$, with $\text{diag}(\cdot)$ denoting a diagonal matrix with entries $(\cdot)$ in the main diagonal, and

$$\begin{aligned} \mathbf{d}_k &= \text{vec}(\mathbf{D}_k), & \mathbf{D}_k &= \{d_{k,ls}\}, & d_{k,ls} &= d_{k+l}[n-s], \\ \mathbf{h}_k &= \text{vec}(\mathbf{H}_k), & \mathbf{H}_k &= \{h_{k,ls}\}, & h_{k,ls} &= h_{k+l}[n-s], \\ \mathbf{w}_k &= \text{vec}(\mathbf{W}_k), & \mathbf{W}_k &= \{w_{k,ls}\}, & w_{k,ls} &= w_{k+l}[n-s], \end{aligned} \tag{8}$$

with $l = -L, \dots, L$, and $s = 0, \dots, S$.

Using the formulation (4), the optimization problem (3) translates into finding the vector $\mathbf{a}_k$ that satisfies

$$\begin{aligned} \frac{\partial}{\partial \mathbf{a}_k} \mathbb{E}\left\{ \left| \hat{h}_k[n] - h_k[n] \right|^2 \right\} &= 2\mathbb{E}\left\{ \mathbf{y}_k \mathbf{y}_k^H \right\} \mathbf{a}_k - 2\mathbb{E}\left\{ h_k^*[n] \mathbf{y}_k \right\} \\ &= \mathbf{0}_{(2L+1)\cdot(S+1)}, \end{aligned} \tag{9}$$

where $\mathbf{0}_m$ denotes the $m \times 1$ all-zero vector. Hence,

$$\mathbf{a}_k = \left[\mathbb{E}\left\{ \mathbf{y}_k \mathbf{y}_k^H \right\} \right]^{-1} \cdot \mathbb{E}\left\{ h_k^*[n] \mathbf{y}_k \right\}. \tag{10}$$

To implement the channel estimation (4) in an iterative fashion, we should investigate how to relate the soft information coming from the decoder with the filter coefficients $\mathbf{a}_k$ computed as in (10). Applying the definitions (7) and (8), we get

$$\mathbb{E}\left\{ \mathbf{y}_k \mathbf{y}_k^H \right\} = \overline{\boldsymbol{\Delta}}_k \cdot \mathbf{R}_\mathbf{h} \cdot \overline{\boldsymbol{\Delta}}_k^H + \mathbf{R}_\mathbf{w}, \tag{11}$$

where $\mathbf{R}_\mathbf{w} = \mathbb{E}\{\mathbf{w}_k \mathbf{w}_k^H\} = \sigma_w^2 \mathbf{I}$ is the correlation matrix of the AWGN noise, with $\mathbf{I}$ denoting the identity matrix, $\mathbf{R}_\mathbf{h} = \mathbb{E}\{\mathbf{h}_k \mathbf{h}_k^H\}$ is the channel correlation matrix, and the matrix $\overline{\boldsymbol{\Delta}}_k = \mathbb{E}\{\boldsymbol{\Delta}_k\} = \text{diag}(\overline{\mathbf{d}}_k)$ contains the *expected* values for the transmitted QAM symbols.

Considering the Fourier transform of the impulse response $h(t)$ defined as in (1) and recalling the statistical independence between different paths, $\mathbf{R}_\mathbf{h}$ can be expressed as

$$\mathbf{R}_\mathbf{h} = \widetilde{\mathbf{F}}^H \cdot \mathbf{R}_\rho \cdot \widetilde{\mathbf{F}}, \tag{12}$$

where

$$\widetilde{\mathbf{F}} = \mathbf{F} \otimes \mathbf{I}_{S+1} \tag{13}$$

with $\mathbf{F} \triangleq [f_{i,l}]_{l=-L,\dots,L}^{i=0,\dots,N_p-1}$, with elements $f_{i,l} = e^{+j2\pi l \Delta f \tau_i}$, $\mathbf{I}_{S+1}$ is the $(S+1) \times (S+1)$ identity matrix and $\otimes$ denotes the Kronecker product, and

$$\mathbf{R}_\rho = \mathbf{R}_\rho^{(f)} \otimes \mathbf{R}_\rho^{(t)} \tag{14}$$

is the correlation matrix of the fading channel, where $\mathbf{R}_\rho^{(f)} = \text{diag}([\sigma_0^2, \dots, \sigma_{N_p-1}^2])$, and $\mathbf{R}_\rho^{(t)} = [R_{u,s}]_{s=0,\dots,S}^{u=0,\dots,S}$, with elements $R_{u,s} = R_\rho((u-s)T_s)$.

Now comes the crucial part of our derivation. The expected symbol values $\overline{\boldsymbol{\Delta}}_k$ are interpreted as *a posteriori* averages and can be computed in real-time using the soft output from the channel decoder. More in detail, $\overline{d}_{k-l}[n-s] \triangleq \mathbb{E}\{d_{k-l}[n-s]\}$ can be obtained exploiting the APP matrices computed by the NB-LDPC decoder on the $(n-s)$th OFDM symbol. Recalling that the decoder operates code block by code block, $\boldsymbol{\Lambda} = [\boldsymbol{\lambda}_0, \dots, \boldsymbol{\lambda}_{N-1}]$, where $\boldsymbol{\lambda}_m$, $m = 0, \dots, N-1$, is a vector containing the APP of each coded symbol $c_m[n-s] \in \mathbf{c}[n-s]$ for any possible symbol b_g, $g = 0, \dots, q-1$ in the GF(q): $\boldsymbol{\lambda}_m = \{\lambda_{m,g}\}_{g=0}^{q-1}$, with $\lambda_{m,g} = \Pr\{c_m[n-s] = b_g \mid \mathbf{y}[n-s]\}$. In general, the QAM constellation order M is different from the Galois field order q. For the sake of brevity, let us assume here that $M = q$ (our results can be extended to the case $M \neq q$ using the methods discussed in [17]). Under this hypothesis, after interleaving and multicarrier modulation, the mapped QAM symbol $d_{k-l}[n-s]$ has a one-to-one correspondence with the GF(q) symbol $c_m[n-s]$. Using the output from the decoder, we can obtain a soft-mapped symbol

$$\overline{d}_{k-l}[n-s] = \sum_{g=0}^{q-1} \lambda_{m,g} \cdot \mu\left(b_g\right), \tag{15}$$

where $\mu(\cdot)$ is the bijective mapping that assigns an M-QAM symbol to a GF(q) coded symbol. In the case of a hard-decision approach, we can replace (15) with

$$\overline{d}_{k-l}[n-s] = \mu(\hat{u}_m), \tag{16}$$

where $\hat{u}_m = b_{g^*(m)}$, with $g^*(m) = \arg\max_g \lambda_{m,g}$.

Using similar manipulations, we can obtain

$$\mathbb{E}\left\{h_k^*[n]\mathbf{y}_k\right\} = \overline{\mathbf{\Delta}}_k \cdot \widetilde{\mathbf{F}}^H \cdot \mathbf{R}_\rho \cdot \widetilde{\mathbf{f}}, \tag{17}$$

where $\widetilde{\mathbf{f}}$ is the central column of the matrix $\widetilde{\mathbf{F}}$.

We now have all the ingredients to provide an estimate $\hat{\mathbf{h}}[n]$ of the channel coefficients according to (4) and (10). The estimation method starts from an initial estimate of the channel coefficients based on pilot subcarriers only. Using this initial estimate, the error-correction decoder decodes the received signal and produces soft information of the coded GF(q) symbols. The iterative process between the channel estimator and the decoder then proceeds by exchanging soft information using a turbo approach. This process constitutes an outer iteration of the turbo architecture sketched in Figure 2, which aims at minimizing the mean-square error of the channel estimate at the expense of an increased complexity in terms of computational power at the receiver. The number of outer iterations (i.e., the number of iterative channel estimation, as opposed to the inner iterations performed by the EMS algorithm at the channel decoder) must be then optimized, as briefly discussed in Section 4.

To reduce the computational demand, we can exploit the properties of the correlation matrices to avoid the explicit real-time inversion of the matrix $\mathbb{E}\{\mathbf{y}_k\mathbf{y}_k^H\}$ as in (10). Since $\mathbb{E}\{\mathbf{y}_k\mathbf{y}_k^H\}$ is a block-Toeplitz matrix, we can use the Levinson-Durbin recursion [18] to significantly reduce the number of operations. To further simplify the computation of the Wiener filter coefficients, we can also apply the Woodbury formula [19] to (10) to get, using (11) and (17),

$$\begin{aligned}\mathbf{a}_k = {}& \left[\overline{\mathbf{\Delta}}_k^H\right]^{-1} \cdot \left[\mathbf{R}_\mathbf{h} + \sigma_w^2\left(\overline{\mathbf{\Delta}}_k^H\overline{\mathbf{\Delta}}_k\right)^{-1}\right]^{-1} \\ & \cdot \left[\overline{\mathbf{\Delta}}_k\right]^{-1} \cdot \overline{\mathbf{\Delta}}_k \cdot \widetilde{\mathbf{F}}^H \cdot \mathbf{R}_\rho \cdot \widetilde{\mathbf{f}}.\end{aligned} \tag{18}$$

In the case of phase shift keying (PSK) (i.e., equal-energy constellations), in which $\overline{\mathbf{\Delta}}_k^H\overline{\mathbf{\Delta}}_k = \mathbf{I}$, (18) can be rewritten as

$$\mathbf{a}_k = \left[\overline{\mathbf{\Delta}}_k^H\right]^{-1} \cdot \boldsymbol{\varphi} \tag{19}$$

with $\boldsymbol{\varphi} \triangleq [\mathbf{R}_\mathbf{h} + \mathbf{R}_\mathbf{w}]^{-1} \cdot \widetilde{\mathbf{F}}^H \cdot \mathbf{R}_\rho \cdot \widetilde{\mathbf{f}}$. Equation (19) shows two interesting properties: (i) it contains the vector $\boldsymbol{\varphi}$, which does not depend on the data, and can thus be computed offline once for ever before filtering starts; and (ii) the data-dependent matrix $[\overline{\mathbf{\Delta}}_k^H]^{-1}$ requires the inversion of a diagonal matrix, thus yielding a negligible impact in terms of computational load. In the case of unequal-energy (e.g., QAM) constellations, the equality in (19) does not hold anymore, and therefore (19) represents a suboptimal solution, whose impact in terms of performance loss with respect to (10) will be evaluated by means of numerical simulations.

As a final remark, it is worth emphasizing that the procedure described above to compute the Wiener filter coefficients (10), using the relations (11) and (17), is valid for *any* coded OFDM transmission over a doubly selective channel. When using a different FEC technique, the only modification in fact occurs in computing the data-dependent matrix $\overline{\mathbf{\Delta}}_k$, whose elements $\overline{d}_k[n]$ (i.e., the expected values of the transmitted symbols) depend on the output of the channel decoder.

4. Simulation Results

The signal format used to evaluate the link-level performance of the iterative estimation is based on the IEEE 802.16e time division duplex (TDD) downlink frame [20]. The relevant system parameters are number of subcarriers $N_s = 1024$, with 720 subcarriers allocated to information symbols and 120 used as pilots, sampling frequency $f_s = 11.2$ MHz, subcarrier spacing $\Delta f = f_s/N_s \simeq 10$ kHz, OFDM symbol duration $T_s = 1/\Delta f \simeq 100\,\mu$s, and carrier frequency $f_0 = 3.5$ GHz. The Galois field order is $q = 64$, and the used parity check matrices are those derived in the FP7-DAVINCI project "Design and Versatile Implementation of Nonbinary Wireless Communications Based on Innovative LDPC Codes" [21]. The encoding scheme adopts a codeword length $N = 360$ and a coding rate 1/2. The I/Q modulation considers an $M = 64$ QAM constellation using standard Gray mapping. The 24-tap ITU modified veh.-A channel profile [22] is considered to model the frequency selectivity, and the Clarke model $R_{\rho_i}(\tau) = \sigma_i^2 \cdot J_0(2\pi f_D \tau)$ is used for the time selectivity, where $J_0(\cdot)$ is the zero-order Bessel function of the first kind. A zero-forcing (ZF) strategy is adopted at the equalizer.

Figure 3 shows the experimental WER as a function of the signal-to-noise ratio (SNR) in terms of energy per symbol E_S and noise power spectral density (PSD) N_0. The relative speed between the transmitter and the receiver is assumed to be $v = 120$ km/h, which yields $f_D \simeq 388$ Hz. The solid line reports the performance of perfect channel state information (CSI), whereas the dashed line represents a fictitious situation in which all the transmitted symbols are known to the receiver (all-pilot case) and are used to perform channel estimation. Wiener filtering in the time domain considering three subsequent OFDM symbols is used to smooth the effects of the noise. Since the only errors affecting the channel estimate are due to the AWGN, this represents some sort of experimental lower bound to the WER performance. The dash-dotted line is obtained using a least-squares pilot-aided method, to serve as an experimental upper bound for the WER performance. Dark and light lines report the results of the proposed solution when soft information and hard decisions are used, respectively. A Wiener filter with $L = 2$ and $S = 2$ is employed. Four different configurations are reported: 3×10 (upper triangles), 3×30 (lower triangles), 6×30 (circles), and 10×30 (square markers), where the first and the second parameter are the number of outer and inner iterations, respectively. As expected, increasing the number of outer and/or inner iterations yields better performance at the expense of an increased computational complexity. Note that in all configurations, the proposed algorithm allows us to reduce the gap with the all-pilot case with respect to the pilot-aided case: in the soft-based scenario, the gap reduces from 1.2 dB to 0.4 dB on average, whereas it becomes about

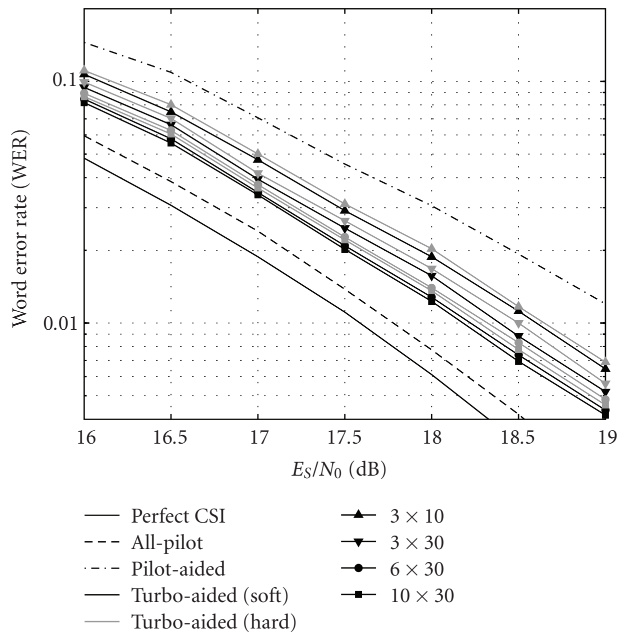

Figure 3: WER performance as a function of E_S/N_0 ($M = q = 64$, $v = 120$ km/h, $L = 2$, and $S = 2$).

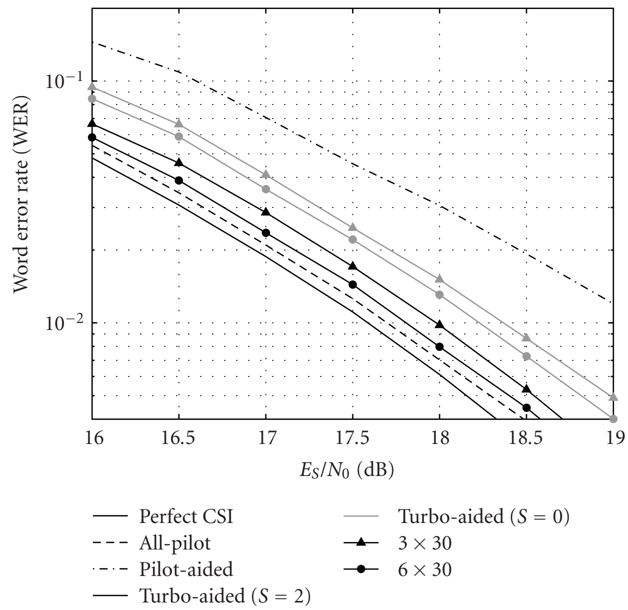

Figure 4: WER performance as a function of E_S/N_0 ($M = q = 64$, $v = 10$ km/h, $L = 2$, variable S, soft information).

0.5 dB in the hard-based case. Interestingly, the performance of hard-directed estimation is quite similar to the soft-based one. We can thus adopt the hard-based approach to reduce the complexity at the expense of an acceptable performance degradation. Note also that a number >6 of outer iterations does not produce substantial WER improvement.

Figure 4 reports the WER performance of the channel estimator when no history is considered ($S = 0$) and when three OFDM symbols are considered to improve the estimation accuracy ($S = 2$). As can be easily argued, the impact of the filter memory S heavily depends on the coherence time of the considered channel. To this aim, we consider a lower relative speed $v = 10$ km/h, which implies a higher coherence time ($f_D \simeq 32.4$ Hz). Dark and light lines depict the cases $S = 2$ and $S = 0$, respectively, when soft information is used. Averaging over three ($S = 2$) channel realizations allows us to reduce the effects of AWGN (the gain is around 0.4 dB). The impact of the channel coherence time is also confirmed by better performance with respect to the $v = 120$ km/h case: when 6 outer iterations are employed, the difference between all-pilot and turbo-aided configurations reduces from 0.4 to 0.1 dB when $S = 2$, whereas it is substantially unchanged when $S = 0$. Note also that when $v = 120$ km/h, using $S = 0$ and $S = 2$ yields almost the same performance due to shorter channel coherence time (the case $S = 0$ is not reported in Figure 3 for the sake of presentation).

In Figure 5, we evaluate the impact of *a priori* knowledge of the channel statistics on the system performance. As emerged from Section 3, (12) requires prerequisite information, such as correlation in time and frequency domain. To this aim, we simulate a scenario in which the channel taps are computed using the 24-tap ITU veh.-A channel model, whereas the 6-tap ITU veh.-A channel model [22] is

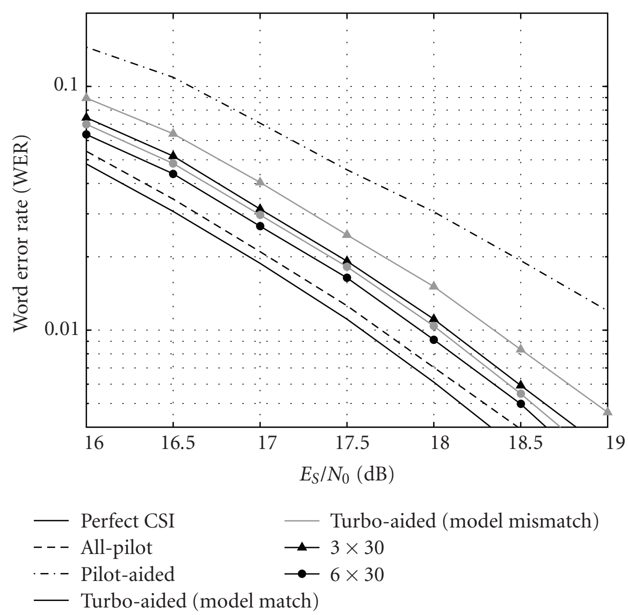

Figure 5: WER performance in the case of imperfect knowledge of *a priori* channel statistics ($v = 10$ km/h, $L = 2$, and $S = 1$).

assumed at the receiver. In this case, the mismatch is mild, since the coherence time is assumed to be known based on the correct Doppler shift, and the coherence bandwidth is similar. However, the average PDP and the number of paths are modified. Figure 5 considers $v = 10$ km/h and a soft-based Wiener filter with $L = 2$ and $S = 1$. In this case, we notice a performance loss of about 0.15 dB and 0.3 dB in the cases 6 × 30 and 3 × 30, respectively.

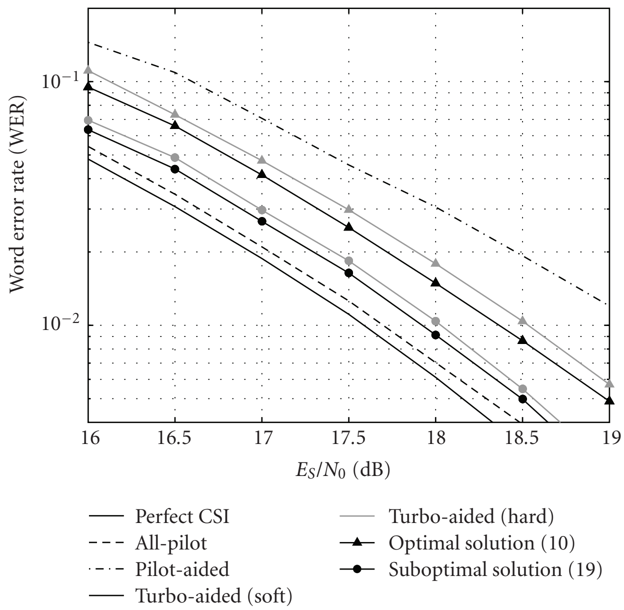

Figure 6: WER performance in the case of suboptimal estimation ($M = q = 64$, $v = 10$ km/h, $L = 2$, and $S = 1$).

Finally, to measure the performance loss of the suboptimal solution (19), Figure 6 compares the WER performance as a function of the SNR. The solution (10), exploiting the joint time-frequency correlation, is shown with circular markers, whereas the suboptimal method (19) is depicted with triangular markers. Both soft-based (dark lines) and hard-directed (light lines) approaches are reported, adopting a Wiener filter with parameters $L = 2$ and $S = 1$, and assuming $v = 10$ km/h. For the sake of presentation, we report here only the case with 6×30 iterations. As can be seen, the loss of the proposed suboptimal solution with respect to the optimal derivation is roughly 0.5 dB. However, it is worth noting that even in the case of the hard-decision approach, the suboptimal iterative solution performs better than the pilot-aided solution, at the expense of a mild increase in the receiver complexity.

5. Conclusion and Perspectives

This paper derived an iterative channel estimation method suitable for OFDM systems with nonbinary LDPC encoding. The proposed approach exploits the channel decoder information, at both soft and hard level to derive a joint time-frequency Wiener filter that minimizes the mean square error of the channel estimate. The novelty of this approach lies in (i) showing how to include the *a posteriori* soft information of any FEC channel decoder in the estimator without resorting to some heuristic formulation and (ii) pairing the turbo estimator with nonbinary LDPC codes, exploiting the properties of q-ary Galois fields and M-QAM constellations.

The benefits of this method have been evaluated using numerical simulations, in which the word error rate (WER) performance as a function of the signal-to-noise ratio (SNR) has been compared to the case of perfect channel knowledge and pilot-aided techniques. Simulation results have shown a significant improvement with respect to the pilot-aided scenario, at the expense of an increased complexity at the receiver. The improvement of turbo techniques versus pilot-aided estimator can be quantified to be about $0.5 \div 1$ dB in terms of SNR. This is especially true for large constellations and with low mobility. In addition, we also noticed that the performance degradation due to channel mismatch and/or hard-detected information and/or suboptimal filtering are *per se* almost negligible when considered individually. The cumulative effect of the three, on the contrary, may degrade the overall performance by a nonnegligible amount.

As a final remark, we observe that the techniques investigated in this paper, evaluated for the downlink of an IEEE 802.16e link, are applicable to the uplink as well. The issue of the additional complexity of turbo techniques is not so stringent for the uplink (since the algorithm would be implemented in the base station) even with today's technology, whilst at the moment the implementation impact for a mobile station must be evaluated versus the potential benefit.

Acknowledgment

This work is supported by INFSCO-ICT-216203 DAVINCI "Design And Versatile Implementation of Nonbinary wireless Communications based on Innovative LDPC codes" (http://www.ict-davinci-codes.eu/) funded by the European Commission under the Seventh Framework Programme (FP7).

References

[1] M. C. Davey and D. MacKay, "Low-density parity check codes over GF(q)," *IEEE Communications Letters*, vol. 2, no. 6, pp. 165–167, 1998.

[2] C. Poulliat, M. Fossorier, and D. Declercq, "Design of regular ($2,d_c$)-LDPC codes over GF(q) using their binary images," *IEEE Transactions on Communications*, vol. 56, no. 10, pp. 1626–1635, 2008.

[3] C. Douillard, M. Jézéquel, C. Berrou, A. Picart, P. Didier, and A. Glavieux, "Iterative correction of intersymbol interference: turbo-equalization," *European Transactions on Telecommunications and Related Technologies*, vol. 6, no. 5, pp. 507–511, 1995.

[4] C. Berrou, J. Hagenauer, M. Luise, C. Schlegel, and L. Vandendorpe, "Special issue on turbo-information processing: algorithms, implementations & applications," *Proceedings of the IEEE*, vol. 95, no. 6, pp. 1146–1149, 2007.

[5] M. C. Valenti and B. D. Woerner, "Iterative channel estimation and decoding of pilot symbol assisted turbo codes over flat-fading channels," *IEEE Journal on Selected Areas in Communications*, vol. 19, no. 9, pp. 1697–1705, 2001.

[6] M. F. Flanagan and A. D. Fagan, "Iterative channel estimation, equalization, and decoding for pilot-symbol assisted modulation over frequency selective fast fading channels," *IEEE Transactions on Vehicular Technology*, vol. 56, no. 4, pp. 1661–1670, 2007.

[7] R. Otnes and M. Tüchler, "Iterative channel estimation for turbo equalization of time-varying frequency-selective

channels," *IEEE Transactions on Wireless Communications*, vol. 3, no. 6, pp. 1918–1923, 2004.

[8] S. Song, A. Singer, and K.-M. Sung, "Soft input channel estimation for turbo equalization," *IEEE Transactions on Signal Processing*, vol. 52, no. 10, pp. 2885–2894, 2004.

[9] X. Nguyen and J. Choi, "Iterative channel estimation and turbo decoding in OFDM systems," in *Proceedings of the IEEE Vehicular Technology Conference*, pp. 166–170, Dallas, TX, USA, September 2005.

[10] Y. N. Lee, A. Ashikhmin, and J. T. Chen, "Impact of soft channel construction on iterative channel estimation and data decoding for multicarrier systems," *IEEE Transactions on Wireless Communications*, vol. 7, no. 7, pp. 2762–2770, 2008.

[11] S. Y. Park, Y. G. Kim, and C. G. Kang, "Iterative receiver for joint detection and channel estimation in OFDM systems under mobile radio channels," *IEEE Transactions on Vehicular Technology*, vol. 53, no. 2, pp. 450–460, 2004.

[12] IEEE 802.16 Broadband Wireless Access Working Group, "IEEE 802.16m System Description Document (SDD)," Tech. Rep., IEEE 802.16m-09/0034r2, September 2009.

[13] 3GPP Technical Specification Group, "Radio Access Network; Evolved Universal Terrestrial Radio Access (E-UTRA); LTE physical layer—general description (Release 8)," Tech. Rep., 3GPP TS36.201 v8.1.0, November 2007.

[14] A. Bourdoux, F. Horlin, E. López-Estraviz, and L. Van Der Perre, "Practical channel estimation for OFDM in time-varying channels," in *Proceedings of the IEEE Global Telecommunications Conference (GLOBECOM '06)*, San Francisco, Calif, USA, November-December 2006.

[15] E. Boutillon and L. Conde-Canencia, "Bubble check: a simplified algorithm for elementary check node processing in extended min-sum non-binary LDPC decoders," *Electronics Letters*, vol. 46, no. 9, pp. 633–634, 2010.

[16] A. Voicila, D. Declercq, F. Verdier, M. Fossorier, and P. Urard, "Low-complexity, low-memory EMS algorithm for non-binary LDPC codes," in *Proceedings of the IEEE International Conference on Communications (ICC '07)*, pp. 671–676, Glasgow, UK, June 2007.

[17] S. Pfletschinger, A. Mourad, E. López, D. Declercq, and G. Bacci, "Performance evaluation of non-binary LDPC codes on wireless channels," in *Proceedings of the ICT Mobile Summit*, Santander, Spain, June 2009.

[18] S. Haykin, *Adaptive Filter Theory*, Prentice-Hall, Upper Saddle River, NJ, USA, 4th edition, 2002.

[19] G. H. Golub and C. F. V. Loan, *Matrix Computations*, Johns Hopkins University Press, Baltimore, Md, USA, 3rd edition, 1996.

[20] IEEE 802.16 Broadband Wireless Access Working Group, "Part 16: air interface for broadband wireless access systems," Tech. Rep., IEEE Std 802.16-2009, May 2009.

[21] DA VINCI Project Team, "DA VINCI: design and versatile implementation of non-binary wireless communications based on innovative LDPC codes," EU-Project INFSCO-ICT-216203, November 2007.

[22] IEEE 802.16 Broadband Wireless Access Working Group, "IEEE 802.16m evaluation methodology document," IEEE 802.16m-08/004r5, January 2009.

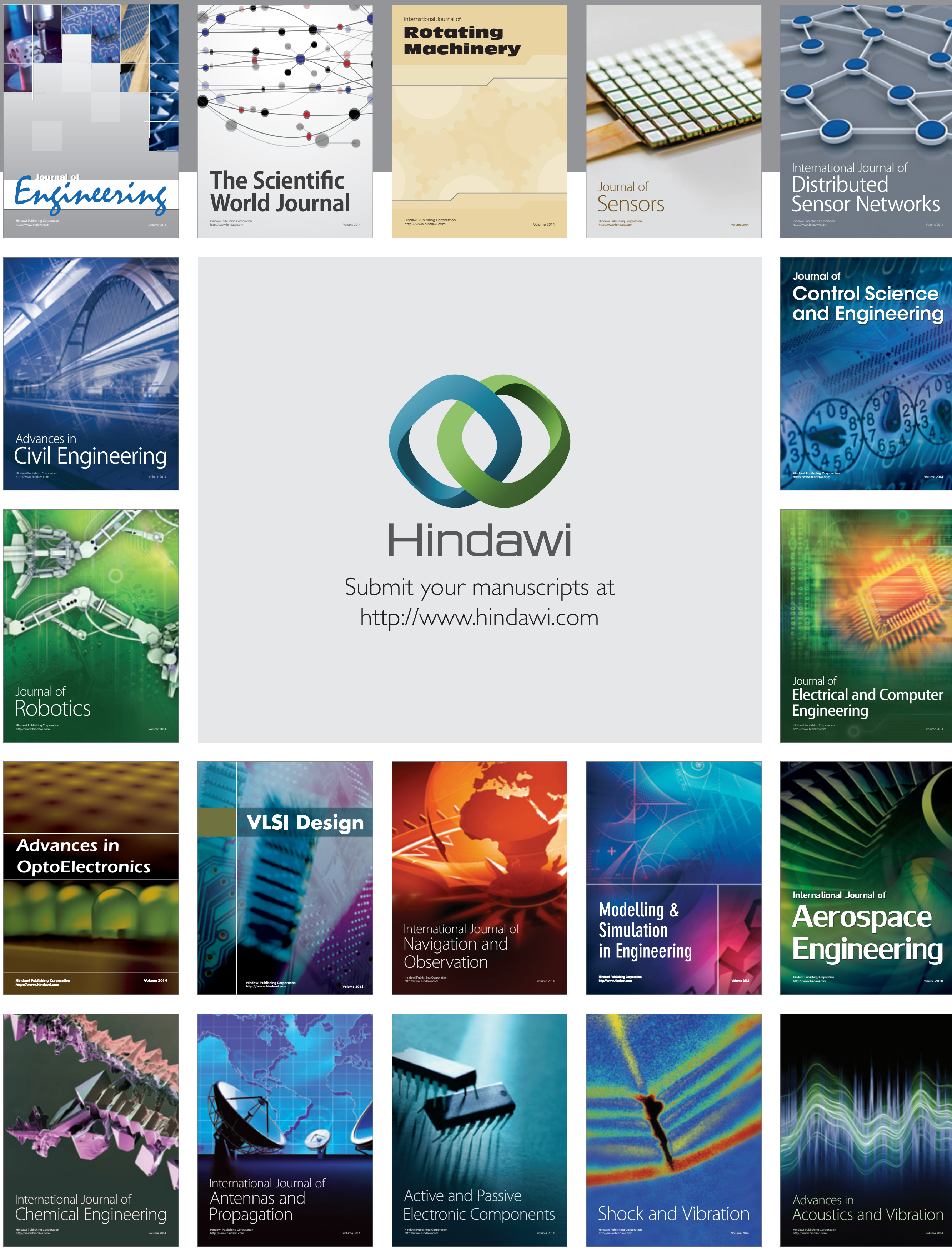

Journal of Engineering
The Scientific World Journal
International Journal of Rotating Machinery
Journal of Sensors
International Journal of Distributed Sensor Networks
Advances in Civil Engineering
Journal of Control Science and Engineering
Hindawi
Submit your manuscripts at
http://www.hindawi.com
Journal of Robotics
Journal of Electrical and Computer Engineering
Advances in OptoElectronics
VLSI Design
International Journal of Navigation and Observation
Modelling & Simulation in Engineering
International Journal of Aerospace Engineering
International Journal of Chemical Engineering
International Journal of Antennas and Propagation
Active and Passive Electronic Components
Shock and Vibration
Advances in Acoustics and Vibration